SAND2022-15669C

Molecular Dynamics Studies of Helium Bubble Effects on Grain Boundary Fracture in $Fe_{70}Ni_{11}Cr_{19}$-1%H Austenitic Stainless Steel

International Conference on Plasticity, Damage & Fracture

Jan. 3-9, 2023, Barcelo Bavaro Punta Cana, Dominican Republic

X. W. Zhou[1], M. E. Foster[1], and R. B. Sills[2]

[1]Sandia National Laboratories, Livermore, California 94550, USA

[2]Rutgers University, Piscataway, New Jersey 08854, USA

Sandia National Laboratories is a multi-mission laboratory managed and operated by National Technology and Engineering Solutions of Sandia, LLC., a wholly owned subsidiary of Honeywell International, Inc., for the U.S. Department of Energy's National Nuclear Security Administration under contract DE-NA-0003525. The views expressed in the article do not necessaril… ment.

Sandia National Laboratories is a multimission laboratory managed and operated by National Technology & Engineering Solutions of Sandia, LLC, a wholly owned subsidiary of Honeywell International Inc., for the U.S. Department of Energy's National Nuclear Security Administration under contract DE-NA0003525.

Motivation

- Stainless steels for nuclear applications develop He bubbles.
- Bubbles promote brittle fracture especially at grain boundaries (GB).
- Improved applications require an understanding of effects on:
  - He bubble areal density on grain boundaries
  - Bubble pressure
  - Temperature
  - Bubble radius
  - Grain boundary types
- **We attempt to use molecular dynamics (MD) simulations to address these problems.**

Approach

- Tensile tests of $Fe_{70}Ni_{11}Cr_{19}$(304L)-1%H with a bubble on GB are simulated.
- Ten GB/cleavage planes are considered: Σ1{111}, Σ3{111}, Σ5{100}, Σ7{111}, Σ9{411}, Σ11{311}, R{100}/{411}, Σ1{100}, Σ1{311}, and Σ1{411}.
- Periodic boundary conditions are used in all three directions.
- Strain controlled simulations with NVT ensemble are used.
- Strain is applied in segments to allow time-averaged energies and stresses to be calculated for each of the segments.
- Various system dimensions ranging from ~200,000 to 700,000 atoms are explored.
- The Fe-N-Cr-H EAM potential in Inter. J. Hydro. Ener., 47, 651 (2022), the He-He and He-metal pair potentials in J. Nuc. Mater., 565, 153753 (2022) are used.

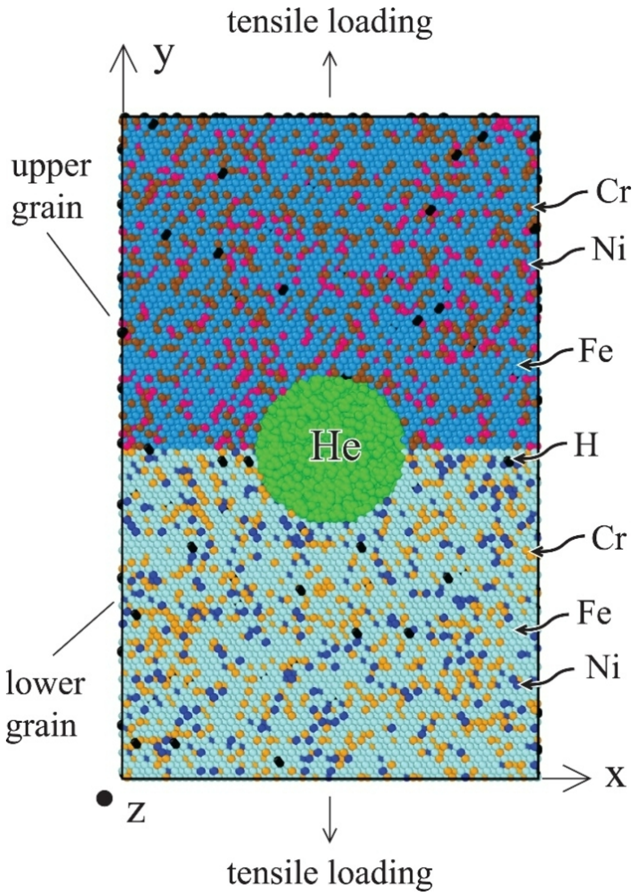

Effects of Accelerated MD Strain Rate

(a) σ vs. ε ***(b)*** ΔE vs. ε

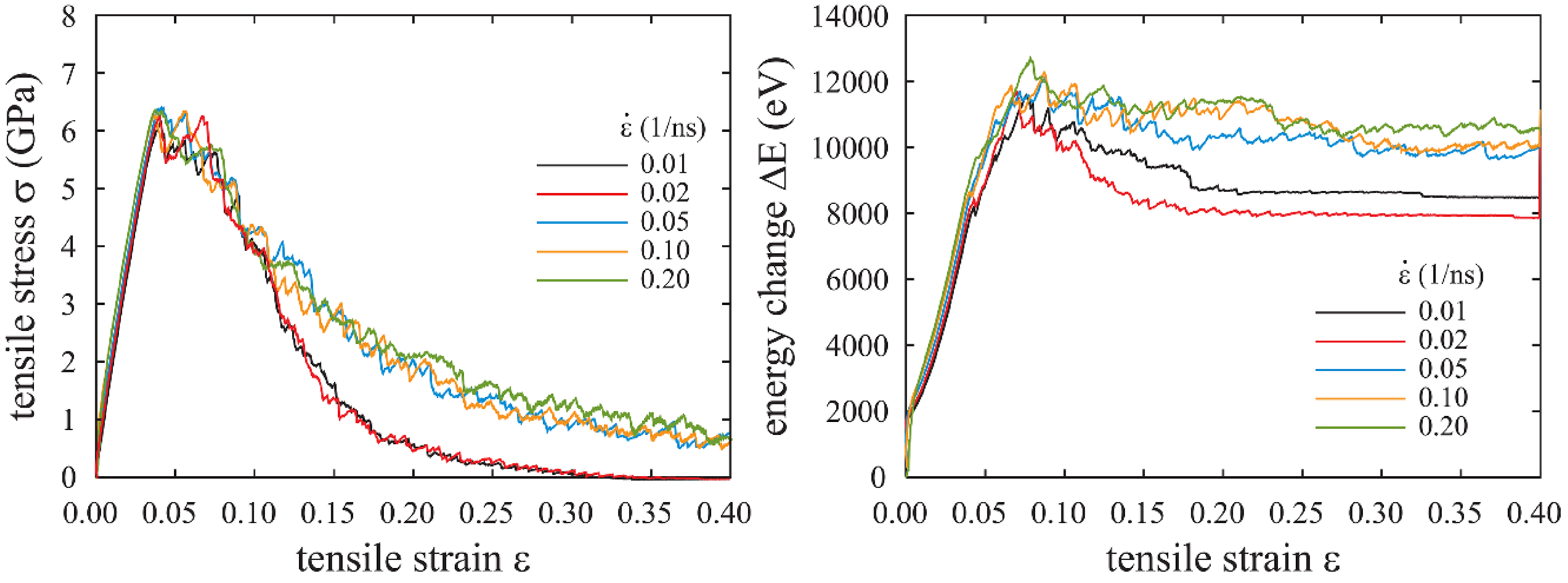

Σ5{100}, system volume V ~ 4600 nm³, interfacial area A ~ 210 nm²
bubble radius r = 3.0 nm, bubble pressure P = 2 GPa, temperature T = 300 K

Large strain rate overshoots stresses and energies. We will use $\dot{\varepsilon} = 0.02$ /ns.

Structures from Low and High Strain Rates

(a) low strain rate of 0.01 (1/ns) ***(b)*** high strain rate of 0.20 (1/ns)

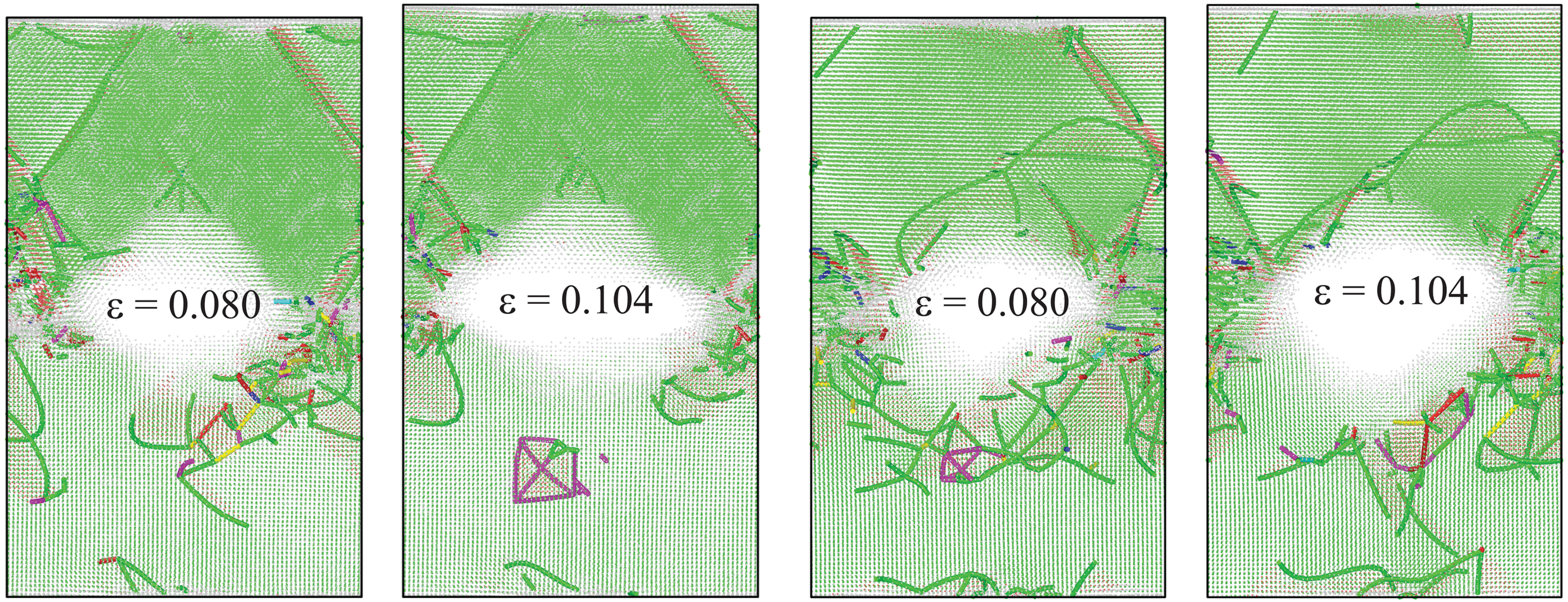

69.2% FCC	71.4% FCC	79.7% FCC	80.6% FCC
281 nm dislocations	208 nm dislocations	367 nm dislocations	357 nm dislocations

—: <110>/2 —: <112>/6 —: <110>/6 —: <001>/3 —: <111>/3 ■: FCC ■: HCP

8 nm slice on x-y plane near bubble, Σ5{100} grain boundary

bubble radius r = 3.0 nm, bubble pressure P = 2 GPa, temperature T = 300 K

Large strain rate overshoots stresses and energies because dislocations do not have time to migrate and annihilate.

Areal Coverage Effects

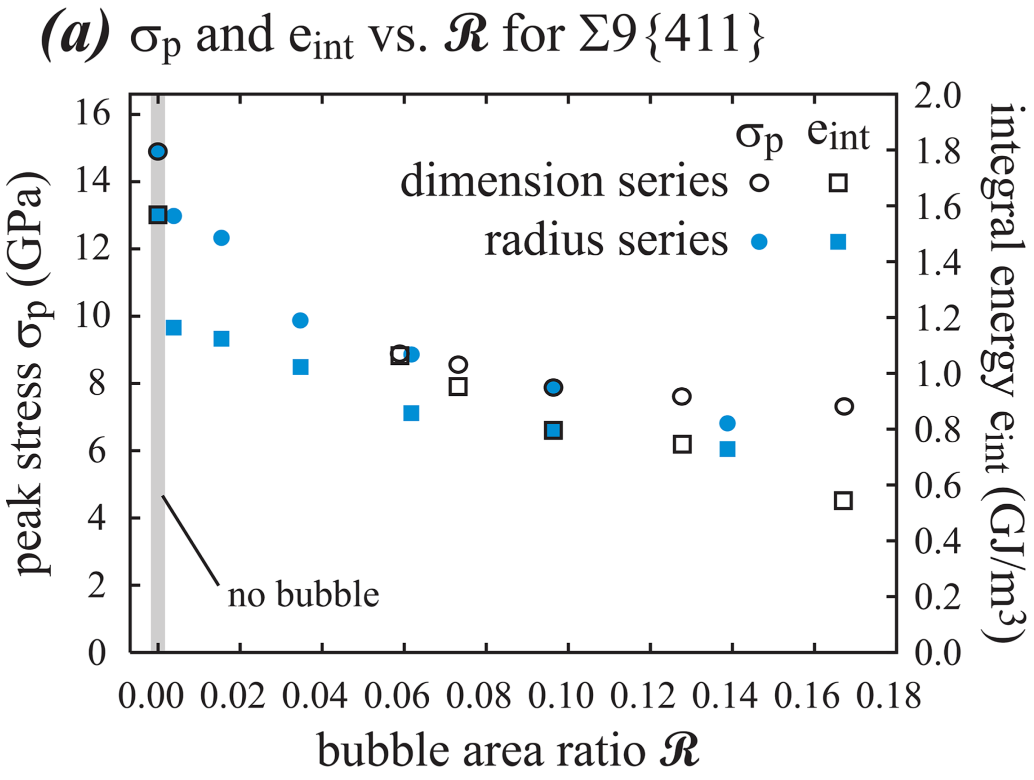

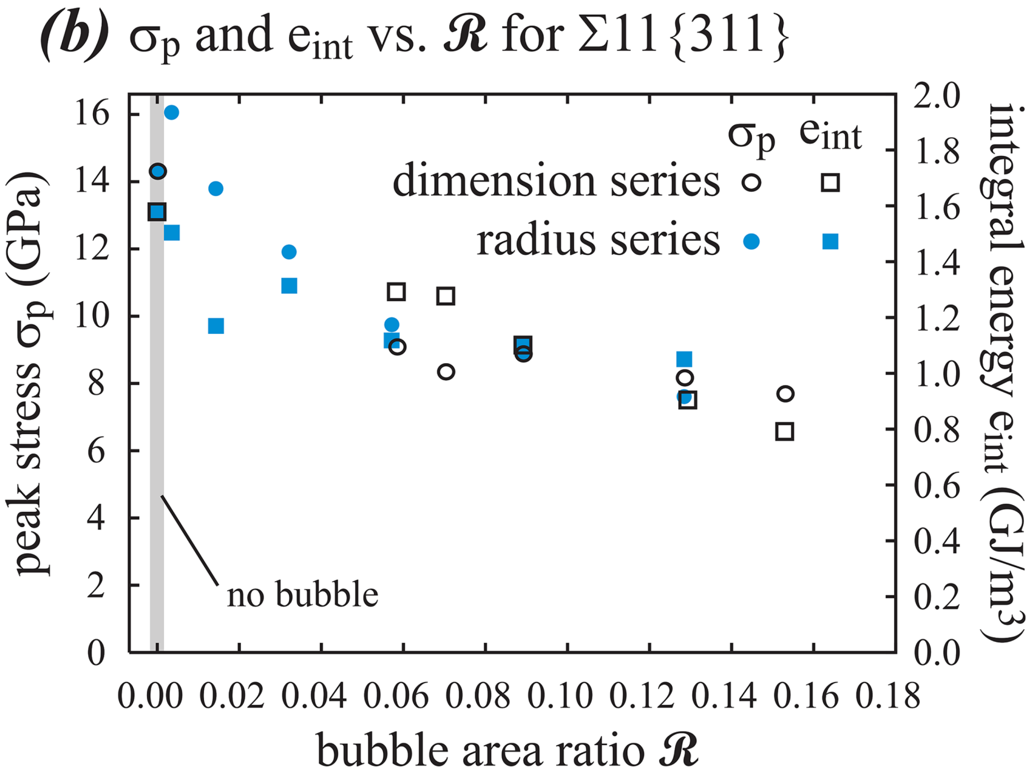

dimension series: bubble radius r = 2.5 nm; radius series: cross section area ~ 15×15 nm^2

bubble pressure P = 2 GPa, temperature T = 300 K, strain rate $\dot{\varepsilon}$ = 0.02 /ns

- Areal ratio can be changed by bubble radius or sample cross section area.
- The peak stress σ_p and integral energy e_{int} both decrease as bubble areal ratio increases.
- With the area effect understood, We will use cross section area ~15X15 nm^2 below.

Bubble Pressure Effects

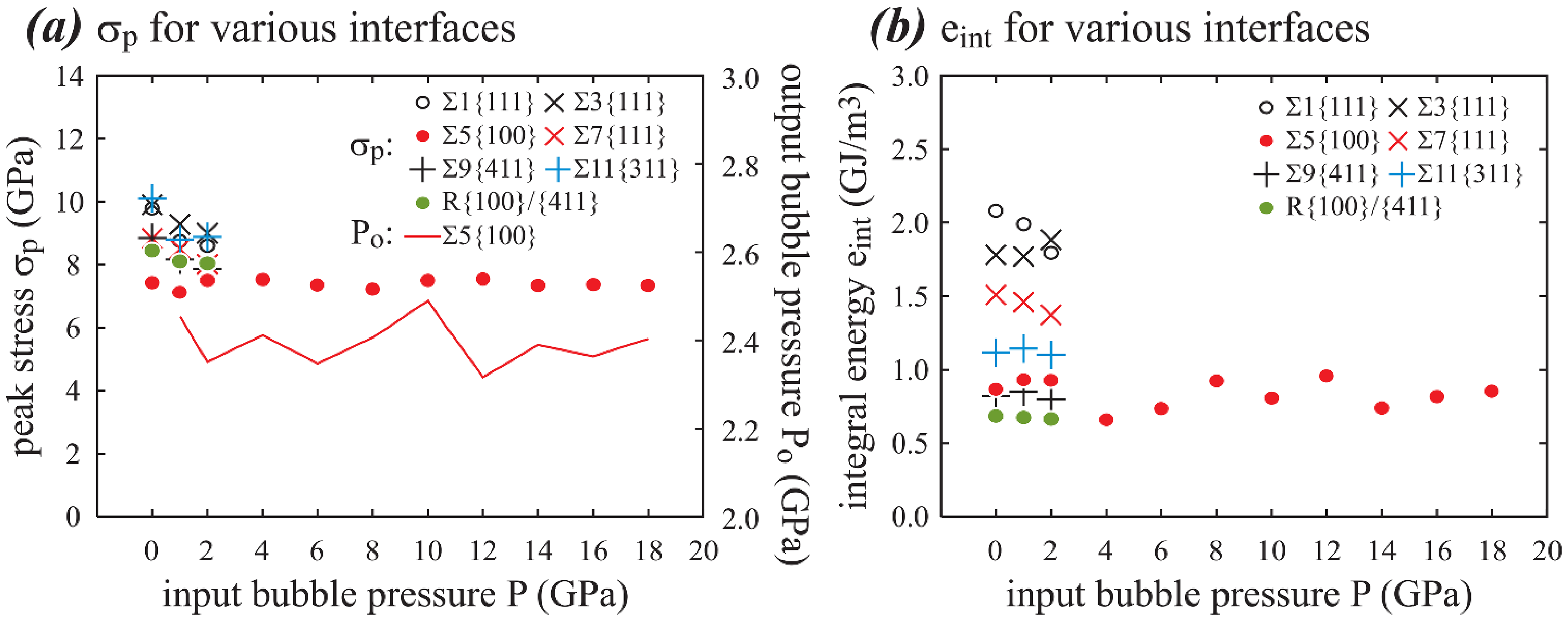

bubble radius r = 2.5 nm, temperature T = 300 K, strain rate $\dot{\varepsilon}$ = 0.02 /ns

- Output pressure remains around 2.4 – 2.6 GPa in the input pressure range 0 – 20 GPa.
- Overall, increasing input pressure from 0 to 2 GPa decreases σ_p and e_{int}.

Temperature Effects

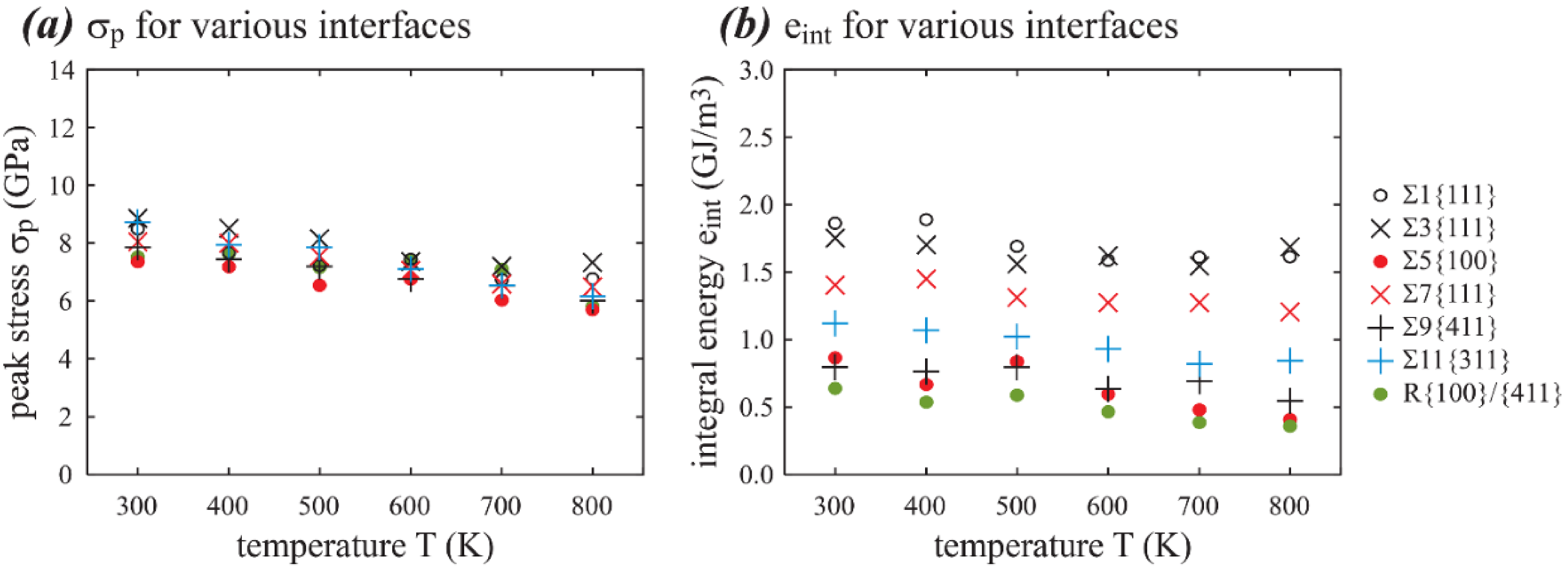

bubble radius r = 2.5 nm, bubble pressure P = 2 GPa, strain rate $\dot{\varepsilon}$ = 0.02 /ns

- Increasing temperature slightly reduces peak stress and integral energy.
- This is consistent with thermally activated nucleation and migration of dislocations.

Bubble Radius Effects

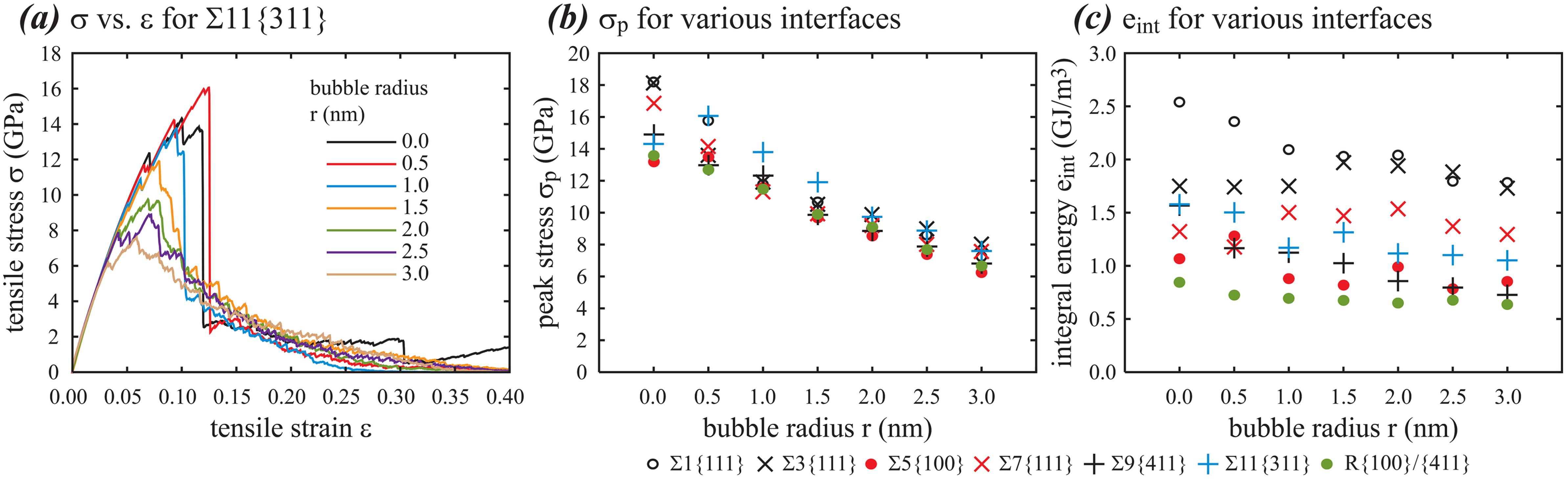

bubble pressure P = 2 GPa, temperature T = 300 K, strain rate $\dot{\varepsilon} = 0.02$ /ns

- ❑ Increasing bubble radius reduces peak stress and integral energy.
- ❑ Areal ratio seems to be more important than bubble radius.

Interface Type Effects

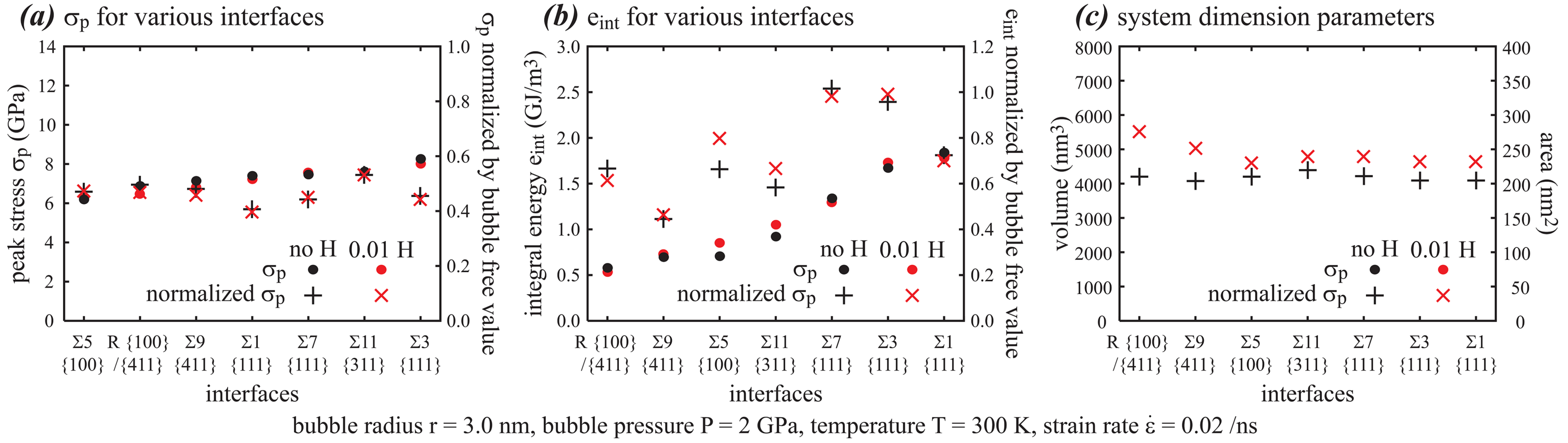

- ❑ σ_p and e_{int} trends are not the same, e_{int} is more reflective of fracture.
- ❑ Interface type more sensitively impacts e_{int}.

Decohesion Energies vs. Interfaces

(averaged over 40 ns)

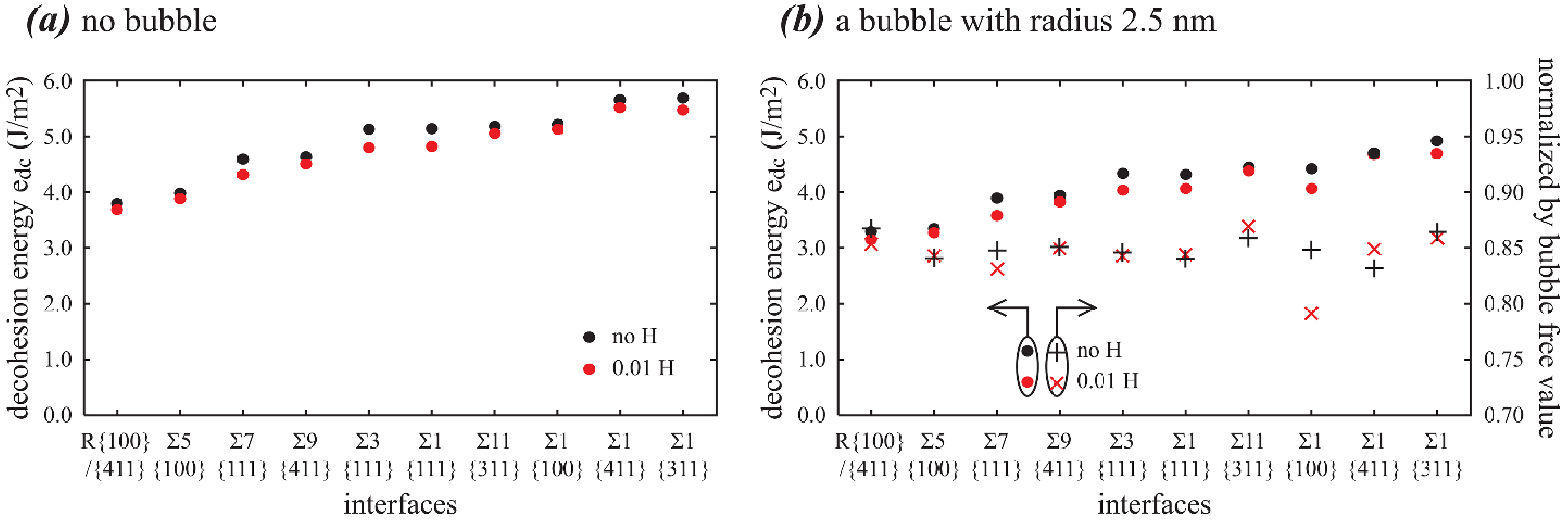

- ❑ Σ1{111} is weaker than Σ11{311}, but the other cleavage planes are all stronger than GB or twin boundaries.
- ❑ The random GB R{100}/{411}has the lowest decohesion energy.

Bubble Effects from All Data

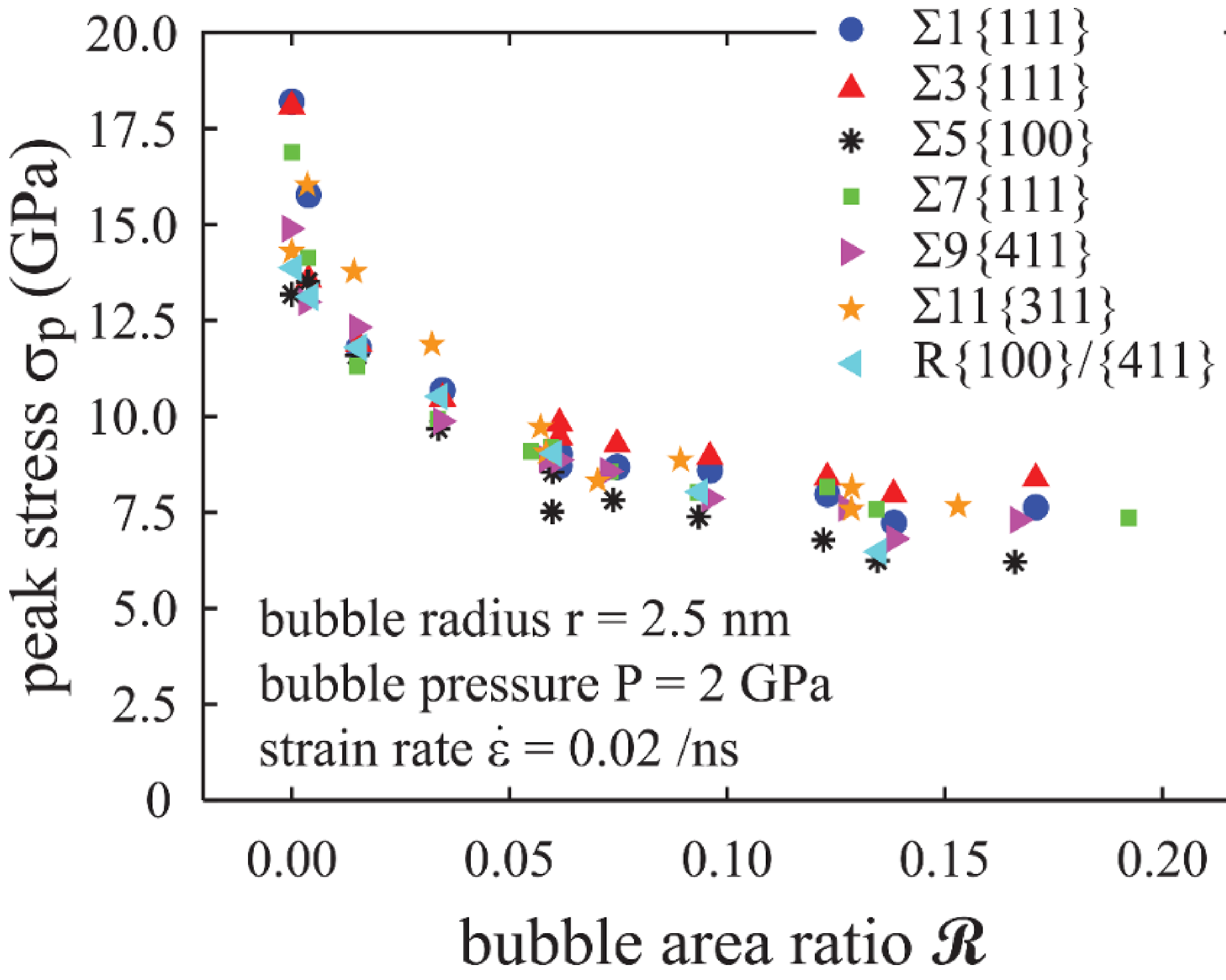

- Peak stress is plotted as a function of areal coverage ratio from both the radius and dimension series for all GBs.
- Peak stress monotonically decreases with areal ratio.

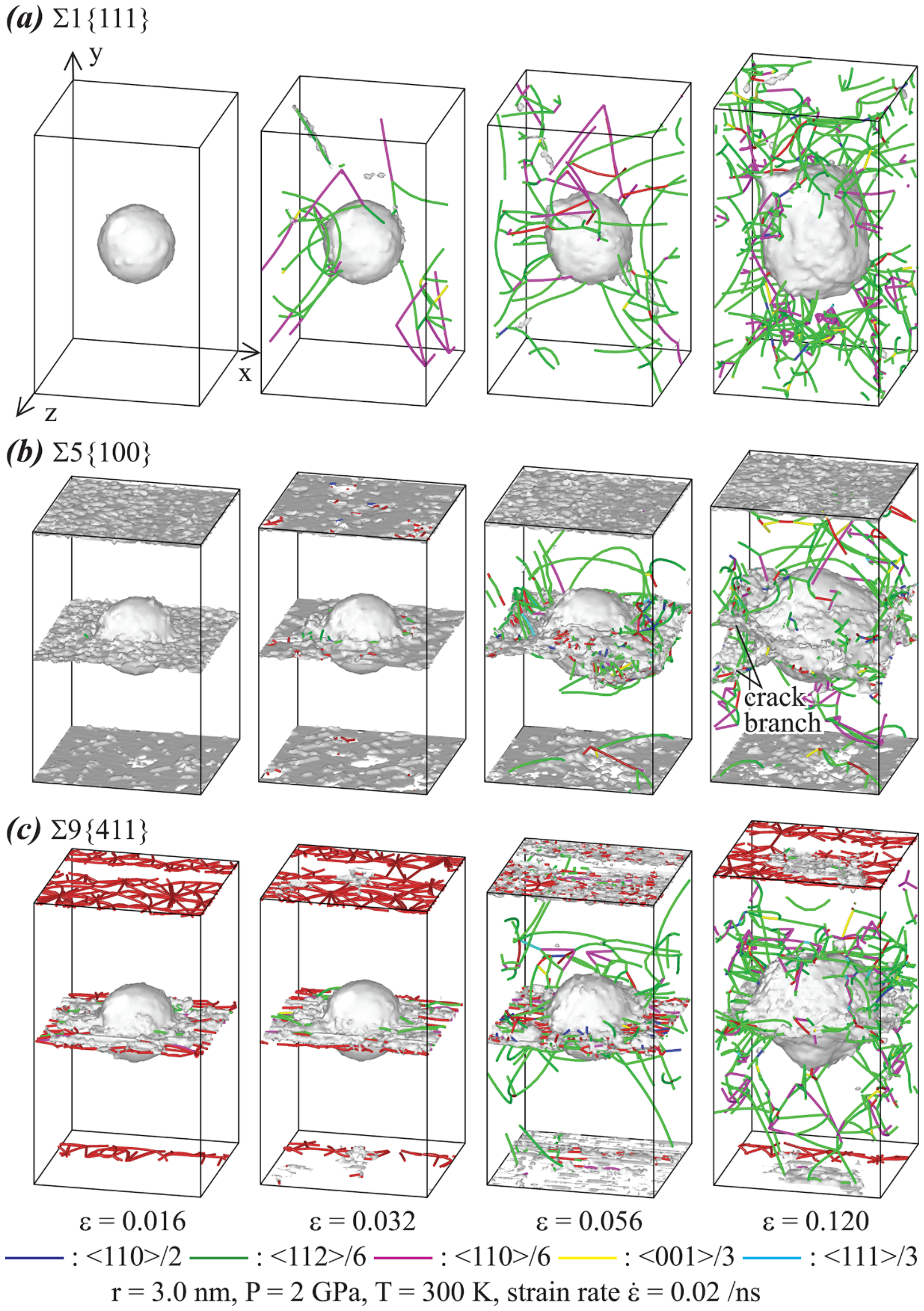

Mechanistic Studies

- Σ1{111} has an intermediate peak stress. Dislocation formation easier?
- Compared with Σ9{411}, Σ5{100} has a higher integral energy but a lower decohesion energy. Why?
- We explored these by visualizing time evolution of atomic configurations.
- Indeed, the Σ1{111} case forms dislocations early.
- The crack branches in the Σ5{100} case causing it to have a high integral energy.

Conclusions

- Fracture energy decreases with increasing bubble areal ratio, bubble pressure, temperature, and bubble radius.
- Initial bubble pressure has little impact on intergranular fracture because it quickly drops once dislocations move.
- The bubble areal ratio has the most important effect on fracture.
- Interface type sensitively impacts fracture. GB more likely causes fracture than cleavage plane. Random GB more likely causes fracture than coherent GB.

Helium Equation of State